

# Excitation–emission fluorimeter based on linear interference filters

Michael Gouzman, Nadia Lifshitz, Serge Luryi, Oleg Semyonov, Dmitry Gavrilov, and Vyacheslav Kuzminskiy

We describe the design, properties, and performance of an excitation–emission (EE) fluorimeter that enables spectral characterization of an object simultaneously with respect to both its excitation and its emission properties. Such devices require two wavelength-selecting elements, one in the optical path of the excitation broadband light to obtain tunable excitation and the other to analyze the resulting fluorescence. Existing EE instruments are usually implemented with two monochromators. The key feature of our EE fluorimeter is that it employs lightweight and compact linear interference filters (LIFs) as the wavelength-selection elements. The spectral tuning of both the excitation and the detection LIFs is achieved by their mechanical shift relative to each other by use of two computer-controlled linear step motors. The performance of the LIF-based EE fluorimeter is demonstrated with the fluorescent spectra of various dyes and their mixtures. © 2004 Optical Society of America

OCIS codes: 300.0300, 300.6190, 300.6280.

## 1. Introduction

In the past two decades the field of fluorescent spectroscopy enjoyed remarkable growth. No longer a mere research tool, it has given rise to a variety of convenient instruments used in many biological applications. This growth has relied on the explosion in data processing techniques and the extensive development of fluorescent probes.

The conventional spectra of fluorescence are either a plot of the intensity of fluorescence of an analyte excited by the light of a fixed wavelength as a function of the emission wavelength or a plot of fluorescence intensity received within a fixed spectral band as a function of the excitation wavelength. These emission and excitation spectra are special cases of a more general three-dimensional representation of fluorescence intensity as a function of both the excitation and the emission wavelengths. The resultant dual excitation–emission (EE) dependency enables spectral characterization of an object simultaneously

with respect to both its excitation and emission. The method offers a fundamental improvement in the sensitivity and reliability of detection, especially when multiple fluorophores are present in the same location.

The three-dimensional representation of fluorescence even from a single-pixel object requires copious amount of data. If either of the two conventional fluorescence descriptions takes  $n$  data points, it is commonly believed that the EE needs  $n^2$  points. This would necessitate a significant increase in the data-acquisition rate, the processing time, and the computer memory. This is probably why all existing devices for the EE analysis are limited to a single-pixel mode (the analyzed object can be macroscopic but uniform over its volume, e.g., a well-mixed sample in a cuvette). We argue, however, that under general conditions one does not need  $n^2$  points,  $2n$  being sufficient for the EE analysis without any loss of information.

The applications of the EE method can be roughly divided into two groups—environmental monitoring tools and biomedical equipment. In the environmental studies, the technique has been widely used for detection of endogenous fluorescence of various chemicals. The biomedical EE equipment can, in turn, be divided into *in vitro* and *in vivo* types. *In vitro* devices are similar to the environmental equipment, whereas *in vivo* devices employ fiber-optic en-

---

The authors are with the Department of Electrical and Computer Engineering, State University of New York at Stony Brook, Stony Brook, New York 11794-2350. The e-mail address for N. Lifshitz is nadia@ece.sunysb.edu.

Received 22 October 2003; revised manuscript received 26 February 2004; accepted 26 February 2004.

0003-6935/04/153066-07\$15.00/0

© 2004 Optical Society of America

doscopy for excitation and emission signal delivery to and out of the tissue under study.

Typically, the EE systems employ two monochromators as the wavelength-selection elements for both the excitation and the emission light. The first monochromator steps up the excitation wavelength. The emission spectrum is scanned with the second monochromator while the excitation wavelength is kept constant.<sup>1–3</sup> Most commercial EE systems are based on such a two-monochromator design and suffer from relatively slow scanning and data acquisition. Significantly shorter EE spectra acquisition times (minutes) can be achieved with a device comprising a monochromator for the selection of the excitation wavelength and a spectrograph to capture the emission spectra, such as an *in vivo* system for interrogation of oral cavity mucosa.<sup>4</sup> Very short acquisition times (seconds) have been demonstrated in experimental spectrofluorimeters with single-measurement EE fluorimetry<sup>5,6</sup> where two spectrographs were used both for excitation and for emission detection from a uniform sample. In this system, a broadband light source irradiated the entrance slit of the excitation spectrograph to spatially disperse the emerged light beam across the sample. The emitted fluorescence was gathered on the entrance slit of the second spectrograph rotated by 90° with respect to the exit slit of the excitation spectrograph. The two-dimensional (2-D) fluorescence data were detected by a CCD or by complementary metal-oxide semiconductor arrays. A drawback of the technique is that it sets stringent requirements to both excitation and detection optics. To the best of our knowledge, there was at least one attempt to market such a spectrofluorimeter.<sup>7</sup> However, when we inquired about the availability of this device, we were told that it had been removed from the market because of technical problems.

In addition to spectral decomposition of broadband light, other methods of tunable excitation have been reported. Often lasers are used as the sources for multiwavelength excitation. For example, a nitrogen–dye laser combination as a tunable excitation source has been used in an *in vivo* endoscope device for gastrointestinal studies.<sup>8</sup> Another sophisticated *in vivo* endoscope system employs a N<sub>2</sub> laser that pumps a sequence of dyes placed on a rotating wheel.<sup>9</sup> Yet another laser-activated tunable wavelength excitation source for pollution analysis<sup>10</sup> employs the effect of frequency doubling and stimulated Raman scattering of a Q-switched Nd:YAG laser to generate many beams of various wavelengths that are separated with a system of prisms and launched into separate optical fibers for conveyance to the sample. In another EE setup, a group of marine scientists used a tunable optical parametric oscillator as a tunable excitation source for macroalgae research.<sup>11</sup> An original solution was found by Naval Research Laboratory scientists<sup>12</sup> who used a set of seven light-emitting diodes (LEDs) within the range between 370 and 636 nm for tunable excitation in their EE assembly.

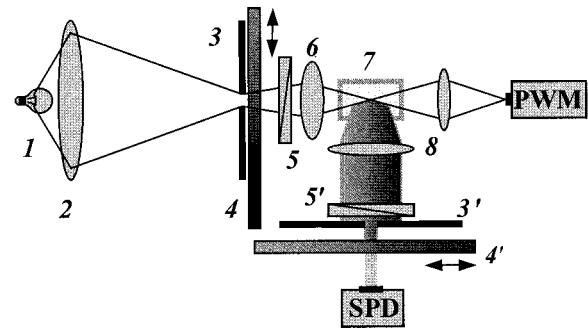


Fig. 1. Schematics of the LIF-based EEF.

These latter EE systems are experimental and custom made for specific applications. All known commercial EE fluorimeters (EEFs) are based on two monochromators and require 2-D scanning. Implementation of the EE method in practical fluoroscopy has been rather narrow so far. In most publications, the technique has been limited to the identification and differentiation of autofluorescence. In spite of its high fluorescence identification ability, it has not yet found its golden application in biological fluorescent detection instruments that differentiate objects labeled with a variety of fluorescent markers. We believe that the fluorescence detection industry shies away from EE fluorescence for three reasons—price, complexity, and weight and size.

An inexpensive, robust, and compact emission wavelength-selection element combined with a broadband or tunable excitation source would stimulate a broader utilization of the EE technique for mainstream fluorescent detection instrumentation. It would be attractive to employ electronically tunable filters. There are several options available today: acousto-optic tunable filters,<sup>13,14</sup> liquid-crystal tunable filters,<sup>15,16</sup> and surface-plasmon<sup>17</sup> tunable optical filters. All these experimental instruments can perform in the EE setup (e.g., the experiments with the EE dye identification were carried out with two acousto-optic tunable filters, one for excitation and another for emission.<sup>13</sup> However, in addition to their specific performance flaws (e.g., high-power consumption for the acousto-optic tunable filter and a low-transmission coefficient for the liquid-crystal tunable filters, these devices depend on a precise modulation of resonant cavities by piezoelectric spacers and hence require a temperature-stabilized environment.

The purpose of this paper is to present a robust and compact EEF based on two linear interference filters (LIFs) as light wavelength-selection elements. LIFs of various sizes and wavelength ranges recently became commercially available. This EEF designed for simultaneous identification of a multiplicity of fluorescent markers in a sample was tested on a variety of dyes and their combinations. The fluorimeter has a single-photon detector (SPD) with a digital output for fluorescence detection.

## 2. Fluorimeter Design

The schematics of the benchtop EEF are shown in Fig. 1. The key feature of the setup is that its wavelength-selection elements are LIFs whose transmittance wavelength varies linearly over the length of the filters. The LIFs are manufactured by Schott and are available from Edmund Optics, Barrington, New Jersey. Their spectral range covers both the visible and the IR regions (400–700- and 400–1000-nm ranges are available) with the light transmission coefficient of 30–45% and the extinction factor for the wavelengths other than in the transmitted range  $\sim 10^4$ . The LIFs come in two sizes, 2.5 cm  $\times$  6 cm and 2.5 cm  $\times$  20 cm and weigh, respectively, 22 and 75 g. In the present experiments, two filters with 2.5 cm  $\times$  20 cm dimensions were chosen to scan the 300–700-nm spectral range.

The excitation arm of the fluorimeter (Fig. 1) consists of a broadband light source 1 (halogen lamp) imaged on a diaphragm 3 with a wide-angle objective 2 to illuminate a quasi-monochromatic region on the excitation LIF 4. The exiting excitation beam of  $\sim 13$ -nm bandwidth is focused into the sample cuvette by an additional lens 6 placed in front of the sample 7. A spectrophotometer or an optical powermeter (PWM is Fig. 1) is used to monitor the intensity and spectrum of the excitation light. The detection arm includes a wide-angle light condenser 8 that directs the quasi-parallel beam on the detection diaphragm 3'. The beam transmitted through the detection LIF 4' is directed to the SPD optical entrance. In addition, two crossed polarizers 5 and 5' are installed in the excitation and emission arms for attenuation of the scattered light.

The spectral tuning of both the excitation and the detection LIFs is achieved by a mechanical shift of the excitation filter relative to the excitation diaphragm and a subsequent mechanical scan of the detection filter relative to the emission diaphragm. The motion and positioning of both filters was regulated by two computer-controlled linear step motors.

### A. Calibration of Linear Interference Filters

Spectral calibration of both LIFs was performed with a spectrophotometer (SP-2000, Ocean Optics, Dunedin, Florida). Figure 2 shows the calibration curves for the excitation and detection LIFs. An example of the spectral distribution of the excitation beam of the first LIF tuned to a wavelength  $\lambda = 525$  nm is shown in Fig. 3. The spectral width of the transmitted band varies from 12.2 nm at the blue edge of the filter (410 nm) to 16 nm at the red edge (720 nm) with an approximately constant half-width of 13 nm in the region between 430 and 580 nm. We found that the spectral band of the transmitted light was virtually independent on the diaphragm width below 2 mm so that a 2-mm-wide diaphragm was chosen to provide the maximum transmitted intensity while the spectral width was kept at a minimum.

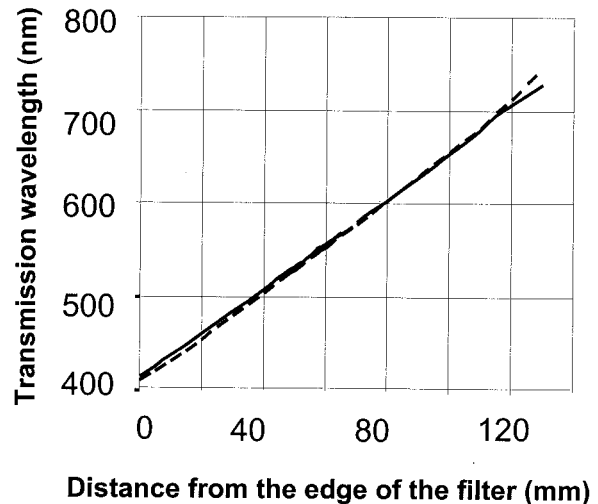


Fig. 2. Calibration curves for two LIFs used in the experiments.

### B. Scattered Light Consideration

In the present setup, the relatively wide spectral width of the excitation beam creates a well-known problem of scattered excitation light that interferes with the fluorescent signal in the detection arm. The scattered light is mostly generated by the Rayleigh scattering of the excitation light on the solvent molecules in the sample cuvette, by impurities dispersed in the solvent, or by a high-concentration dye. To minimize the intensity of scattered light in the detection channel, a system of two crossed polarizers with a contrast ratio of  $\sim 10^2$  each was installed as shown in Fig. 1. In practice, the scattered signal does not influence the measurements of the fluorescent spectrum with the exception of a narrow region where the excitation and emission wavelength are close. The effect becomes more significant at a low concentration of dyes when the fluorescent light intensity becomes comparable with the intensity of scattered light.

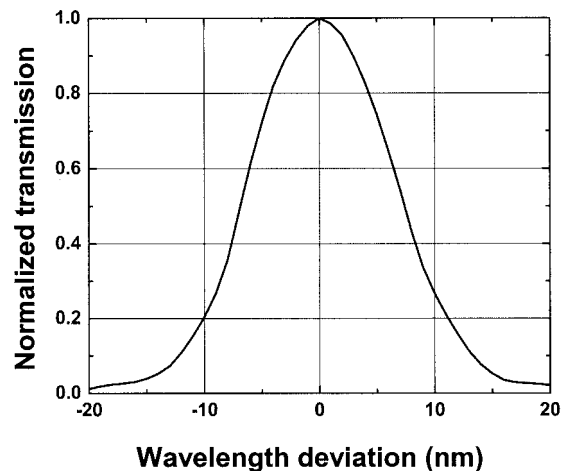


Fig. 3. Spectral distribution of the excitation LIF.

The scattered light was accounted for by our software as we describe in Subsection 2.C.

### C. Data Collection and Processing

The data collection was controlled by a PC-based control module. The module initiates a series of measurements of the fluorescence intensity by selecting the emission and excitation wavelength bands for each measurement in accordance with a specified data collection scheme that determines how the samples of the spectra will be distributed across the EE plane. The data collection schemes fall into two categories: with uniform sampling and with nonuniform sampling. Although uniform sampling is useful when no *a priori* knowledge about the EE spectrum is available, several optimized schemes with a reduced number of sample points and data collection times can be applied when some *a priori* information exists, allowing for an appropriate choice of nonuniformly sampled data. For example, the sampling density can be increased in those areas of the EE plane where the magnitude of the data gradient exceeds a certain level.

A set of measurements resulting from the experiment is processed by the data processing software. To improve data quality and simplify data presentation, the data undergoes resampling and deconvolution. The resampling positions the data at the nodes of a regular grid on the EE plane while choosing the grid size to incorporate the finest features of the EE spectrum. We obtain the new data by approximating the region of the experimental EE spectrum with spline functions and evaluating EE values at the new nodes based on the approximation. The deconvolution procedure (2-D modification of the Jansson method<sup>18</sup>) is applied to the resampled data to reduce blurring due to the relatively wide bandpass of the LIFs. On the basis of the experimentally measured blurred data and known characteristics of the excitation and emission filters, the estimates of the reconstructed deblurred data are generated. The iterative procedure optimizes the estimates by minimizing the mean-square deviation of the convolution with the filter characteristics from the original blurred data.

One of the functions of the software was to account for the scattered light. Its intensity is measured at the edges of the  $(\lambda_{exc}, \lambda_{em})$  2-D space where the excitation wavelength is sufficiently far from the emission wavelength and the fluorescent signal is substantially weaker than the scattered signal. We found that the amplitude of the detected scattered signal increases with the wavelength following the spectral characteristic of the lamp (linear in the 400–700-nm range) and has a half-width corresponding to the half-width of the excitation beam. Armed with these facts, we could interpolate the shape and magnitude of the scatter into the area of overlapped emission and scattered light signals. For each data point, the magnitude of the scattered intensity is calculated and subtracted from the measured total light intensity at a given spectral point.

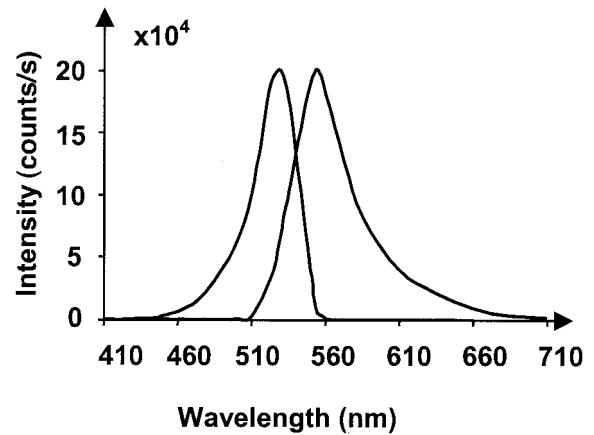


Fig. 4. Excitation and emission spectra of a  $10^{-8}$ -M solution of Rhodamine 6G obtained with the EEF.

## 3. Experimental Results

### A. Experimental Excitation–Emission Spectra

The performance of the setup to detect fluorescence markers was studied with a number of fluorescent dyes dissolved in water and placed in a 1 cm  $\times$  1 cm  $\times$  1 cm sample cuvette. Figure 4 exhibits conventional excitation and emission spectra of a  $10^{-8}$ -M solution of Rhodamine 6G (Exiton, Dayton, Ohio) measured in our setup. Comparison with the standard curves obtained with a monochromator showed no significant differences in the spectra. The three-dimensional image of the EE spectrum obtained with a  $10^{-9}$ -M solution of the same dye is shown in Fig. 5. A scan of the Cy3 dye (Amersham Biosciences) emission spectrum (Fig. 6) reveals all the spectral details; the spectrum is only slightly smoothed in comparison with the monochromator scan of the same dye excited by a laser. Thus the transition from the narrow-band excitation and detection scheme (laser plus monochromator) to the 13-nm bandwidth is not detrimental to the spectral resolution.

To demonstrate the ability of our method to distinguish between different dyes of strongly varied abun-

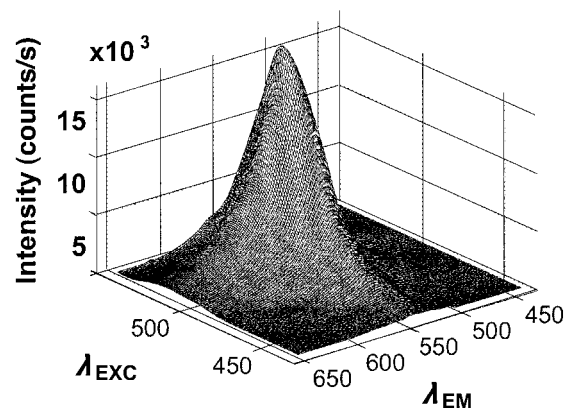


Fig. 5. EE spectrum of a  $10^{-9}$ -M Rhodamine 6G solution obtained with the EEF.

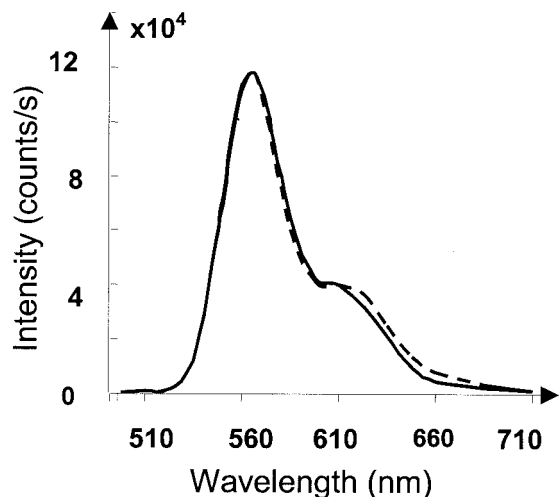


Fig. 6. Two Cy3 dye emission spectra. Dashed curve: monochromator scan of the dye excited by a laser. Solid curve: excitation and detection by two LIFs with our EEF.

dance, we experimented with mixtures of two dyes. Figures 7(a) and 7(b) display the 2-D EE spectra obtained with mixtures of Cy2 and Cy3 dyes with concentration ratios of 10 to 1 and 1 to 6. In spite of the significant differences in concentration, both dyes are distinctly separated in the plots and can be easily identified and quantified. This experiment demonstrates the power of the EE technique. A conventional fluorescence scan could not detect the presence of the lower-concentration dye in Fig. 7(a).

#### B. Evaluation of the Efficiency of the Optical Setup

The main goal of the experiments described above is to demonstrate the feasibility of the LIFs as the light wavelength selector in the fluorimeter assembly rather than the optimization of its optical throughput. However, it is important to estimate the total losses in the system and determine where the heaviest losses occur. The optical throughput of the system is the product of losses at various elements in the optical path. The fluorescent response of the system also factors in the efficiency of the fluorescent excitation. In Subsections 3.B.1 and 3.B.2 we evaluate the losses and throughput and compare them with the experimental results.

##### 1. Throughput of the Excitation Arm

Elements of the excitation optics (Fig. 1) include a halogen lamp, a wide-angle optical condenser, a diaphragm to fit the excitation beam into a rectangular shape, an excitation LIF, a polarizer, and a focusing lens. We calculated the parameters necessary to estimate the optical loss such as stereographic angle of light collection by the condenser and the ratio of the diaphragm area to the area of the source image on the diaphragm. With known values of the LIF transmission coefficient, the polarizer transmission factor, and the reflections from the air-glass optical boundaries, we estimated the

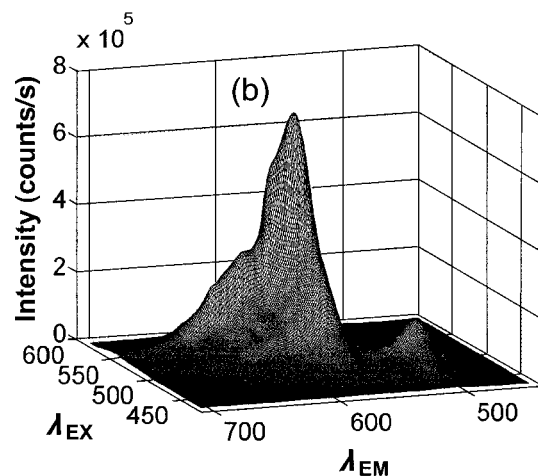
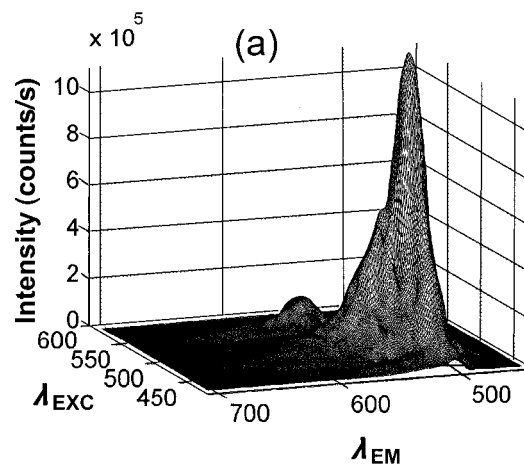


Fig. 7. EE spectra of mixtures of Cy2 and Cy3 dyes: (a) concentration ratio 10 to 1 and (b) concentration ratio 1 to 6.

throughput of the excitation arm  $K_{\text{exc}}$  to be equal to  $4.2 \times 10^{-4}$ . This is similar to the throughput of a single monochromator.<sup>19</sup>

##### 2. Throughput of the Detection Arm

Elements of the detection optics include a condenser, a detection diaphragm, a detection LIF, a detection polarizer, and a SPD. We calculated the parameters necessary to estimate the optical loss such as the stereographic angle of the fluorescent collection, the ratio of the diaphragm area to the area of the fluorescent image on the diaphragm, and the ratio of the SPD input area to the fluorescent beam cross section. Knowing the LIF transmission factor, the transmission of the detection polarizer, the SPD efficiency, and the reflections from the air-glass boundaries, we estimated the throughput of the detection arm  $K_{\text{det}}$  to be equal to  $4 \times 10^{-6}$ . The losses in the detection arm exceed those in the excitation arm by 2 orders of magnitude; 1 order of magnitude was added by the geometric loss factors (smaller stereometric collection angle, ratio of the SPD input area to the fluorescent

beam cross section); another factor of 10 is due to the 10% SPD efficiency.

To reconcile the calculated efficiency with the experimental results, we have to factor in the efficiency of the fluorescent excitation. Considering, for example, the experiment with the  $10^{-9}$ -M Rhodamine sample (Fig. 5) with the peak of the measured fluorescent signal  $N_F \sim 20,000$  counts/s, we can compare it with the value calculated from known parameters of the dye and optical throughput of the setup. The efficiency of the fluorescent excitation, that is, the ratio of the number of fluorescent photons per second  $N_F$  emitted from an observed volume to the number of excitation photons per second  $N_I$  incident to the volume, can be calculated from the following expression<sup>20</sup>:

$$N_F/N_I = \Phi n \sigma d. \quad (1)$$

Here  $\Phi$  is the quantum yield (close to unity for Rhodamine 6G<sup>21</sup>);  $n$  is the dye density ( $6 \times 10^{11} \text{ cm}^{-3}$  for a  $10^{-9}$ -M concentration of Rhodamine 6G);  $\sigma$  is the absorption cross section in square centimeters [ $\sigma = 3.8 \times 10^{-21} \times \epsilon$ , where  $\epsilon$  is the dye molar extinction coefficient ( $\epsilon = 10^5$  for Rhodamine 6G at the maximum of excitation spectrum<sup>22</sup>)]; and  $d$  is the length of the observed volume (volume of fluorescent radiation gathered by the lens and limited by the diaphragm in the detection arm) along the direction of the excitation beam. Substituting all parameters, we find  $N_F/N_I = 5.2 \times 10^{-5}$ , and the expected fluorescent response of the system  $R_F$  is the product  $K_{\text{exc}} K_{\text{det}}$   $N_F/N_I = 4.2 \times 10^{-4} \times 4 \times 10^{-6} \times 5.2 \times 10^{-5} = 8.3 \times 10^{-14}$ .

The number of the incident excitation photons was estimated as follows. We calculated that the lamp radiated  $\sim 0.18$  W within the 13-nm linewidth band or, translated into the number of photons (at 550 nm),  $N_{550}$ ,  $\sim 5 \times 10^{17}$  photons/s. Multiplying this by the fluorescent response  $R_F$  we obtain the expected signal as  $5 \times 10^{17} \times 8.3 \times 10^{-14} = 4 \times 10^4$  counts/s, a remarkably good agreement with the 20,000 counts/s measured experimentally. This result ascertains that the estimation of the EEF efficiency accounts for all major losses.

#### 4. Discussion

Results obtained on our simple experimental setup indicate that it is feasible to implement an inexpensive, lightweight, and robust LIF-based fluorimeter. Most of the losses was due to the poor collection of the excitation light and the fluorescence by inefficient optics. Nevertheless, our assembly demonstrated the ability to confidently detect and quantify the EE spectra of dyes with the molar concentration down to  $10^{-9}$  and to quantitatively distinguish dyes with vastly different concentrations present at the same location. We believe that several easily achievable improvements in the system such as use of light sources with higher luminosity, maximization of the diaphragm area, an increase in the collection angle of excitation and detection condenser, and the fitting of

the shapes of the light source and the fluorescing volume to the geometry of excitation and detection diaphragms can increase its sensitivity by at least 2 orders of magnitude.

Our system employs two LIFs, one for creating tunable excitation and the other for analysis of the fluorescence. The operation of the EEF thus requires coordinated mechanical scanning of both filters. In the present design, both LIFs are moved on rails by two linear step motors. In future designs, to ensure the longevity of moving parts, it will be prudent to use frictionless magnetic floating platforms with programmable linear motion systems. To reduce or completely eliminate mechanical scanning, the fluorimeter should employ an alternative source of tunable excitation while still relying on the detection LIF for analysis of fluorescence.

Finally, we would like to comment on the fundamental information and theoretic question associated with the EE method in general. The physics of fluorescence is such that the shape of fluorescent spectra is to a good approximation independent of the way the dye molecule has been excited. This means that the joint distribution corresponding to the signal  $S$  ( $\lambda_{\text{exc}}, \lambda_{\text{em}}$ ) should be factorizable into a product of distributions  $S_1(\lambda_{\text{exc}})$  and  $S_2(\lambda_{\text{em}})$ , and consequently the entire EE spectrum, when properly parameterized, should be describable by  $2n$  data points to the same resolution as the conventional fluorescence emission, and the fluorescence excitation spectra are described with  $n$  points. This observation should become critical for the development of EE-based fluorescent imaging devices beyond a single pixel.

#### 5. Conclusion

A benchtop prototype of an EEF based on commercially available LIFs as light wavelength-selection elements was developed and the feasibility and performance of the LIFs was tested. We verified the performance of the fluorimeter by obtaining 2-D EE spectra of several fluorescent dyes of different molar concentrations and their mixtures. In the course of this study, we spectrally calibrated the filters and found the algorithm to account for the scattered light. We optimized the spectral characteristics of the pseudo-monochromatic excitation and developed a data processing for resampling and deconvolution techniques that minimizes the data blurring due to the finite wavelength range of the excitation.

#### References and Notes

1. I. M. Warner, G. D. Christian, and E. R. Davidson, "Analysis of multicomponent fluorescence data," *Anal. Chem.* **49**, 564–573 (1977).
2. P. R. Rava, R. Richards-Kortum, M. S. Feld, and J. J. Baraga, "Contour mapping of spectral diagnostics," U.S. patent 5,345,941 (13 April 1993).
3. K. J. Albert and D. R. Walt, "High-speed fluorescence detection of explosives-like vapors," *Anal. Chem.* **72**, 1947–1955 (2000).
4. A. Zuluaga, U. Utzinger, A. Durkin, H. Fuchs, A. Gillenwater, R. Jacob, B. Kemp, J. Fan, and R. R. Richards-Kortum, "Fluorescence excitation-emission matrices of human tissues: a

- system for in vivo measurements and method of data analysis," *Appl. Spectrosc.* **53**, 302–311 (1999).
5. A. R. Muroski, K. S. Booksh, and M. L. Myrick, "Single measurement excitation emission matrix spectrofluorometer for determination of hydrocarbons in ocean water," *Anal. Chem.* **68**, 3534–3538 (1996).
  6. R. D. Jiji, G. A. Cooper, and K. S. Booksh, "Excitation-emission matrix fluorescence based determination of carbamate pesticides and polycyclic and aromatic hydrocarbons," *Anal. Chim. Acta* **397**, 61–72 (1999).
  7. SPEX-3D from Jobin-Yvon, information available at <http://www.jobinyvon.co.uk/jy/fluorescence/fluorescence.htm#>.
  8. R. Richard-Kortum, L. Tong, and M. S. Feld, "Spectral diagnosis of diseased tissue," U.S. patent 5,421,337 (6 June 1995).
  9. R. A. Zangaro, L. Silveira, R. Manochoran, G. Zonios, I. Itzkan, R. R. Dasari, J. Van Dam, and M. S. Feld, "Rapid multiexcitation fluorescent spectroscopy for *in vivo* tissue diagnostics," *Appl. Opt.* **35**, 5211–5219 (1996).
  10. J. E. Kenny, "Laser fluorescence EEM probe for cone penetrometer pollution analysis," EPA/600/R-99/041 (U.S. Environmental Protection Agency, Office of Research and Development, Washington, D.C., 1999).
  11. C. Kieleck, B. Bousquet, G. Le Brun, J. Cariou, and J. Lotrian, "Laser induced fluorescent imaging: application to groups of macroalgae identification," *J. Phys. B* **34**, 2561–2571 (2001).
  12. S. J. Hart and R. D. Jiji, "Light emitting diode excitation emission matrix fluorescence spectroscopy," *Analyst* **127**, 1693–1699 (2002).
  13. C. D. Tran and R. J. Furlan, "Spectrofluorometer based on acousto-optics tunable filter for rapid scanning of multicomponent sample analysis," *Anal. Chem.* **65**, 1675–1681 (1993).
  14. J. Romier, J. Selves, and J. Gastellu-Etchegorry, "Imaging spectrometer based on acousto-optics tunable filter," *Rev. Sci. Instrum.* **69**, 2859–2867 (1998).
  15. K. J. Zuzak, M. D. Schaeberle, E. N. Lewis, and I. W. Levin, "Visible reflectance hyperspectral imaging: characterization of a noninvasive, in vivo system for determining tissue perfusion," *Anal. Chem.* **74**, 2021–2028 (2002).
  16. H. R. Morris, C. C. Hoyt, and P. J. Treado, "Imaging spectrometers for fluorescence and Raman microscopy—acoustooptic and liquid crystal tunable filters," *Appl. Spectrosc.* **48**, 857–866 (1994).
  17. S. D. Russell, R. L. Shimabukuro, A. D. Ramirez, and M. G. Lovern, "Surface plasmon tunable filter for multiband spectral imaging," in *SPAWAR Systems Center Biennial Review* (Space and Naval Warfare Systems Center, San Diego, Calif., 2001), pp. 117–121.
  18. P. A. Jansson, ed., *Deconvolution with Applications in Spectroscopy* (Academic, New York, 1984), p. 342.
  19. See calculations of the throughput of a monochromator, Oriel manual (Oriel Instruments, Stratford, Conn., 2003), pp. 4–13.
  20. A. P. Larson, H. Ahlberg, and S. Folestad, "Semiconductor laser-induced fluorescence detection in picoliter volume flow cells," *Appl. Opt.* **32**, 794–805 (1993).
  21. C. V. Bindhu, S. S. Harilal, V. P. N. Nampoori, and C. P. G. Vallbhan, "Solvent effect on absolute fluorescence quantum yield of Rhodamine 6G determined using transient thermal lens technique," *Mod. Phys. Lett. B* **13**, 563–574 (1999).
  22. DNA Technology Technical Bulletin, "Fluorescence excitation and emission," [www.idtdna.com/program/techbulletins/Fluorescent\\_Dye\\_Labeled\\_Oligonucleotides.asp](http://www.idtdna.com/program/techbulletins/Fluorescent_Dye_Labeled_Oligonucleotides.asp).